

Article

Effect of Calcium and Ectomycorrhiza Collaboration on Nitrogen Nutrition and Rhizosphere Microbial Community of *Pinus massoniana* L. Container Seedlings

Li Pang ^{1,*}, Yunpeng Wang ², Zhiwei Qiao ¹, Wenyang Zhou ¹ and Chao Liu ³

¹ College of Agriculture, Anshun University, Anshun 561000, China; qiaozhiweiwode@163.com (Z.Q.); biozhouwenyang@126.com (W.Z.)

² Institute of Biological Resources, Jiangxi Academy of Sciences, Nanchang 330096, China; wycnsd@163.com

³ College of Resources and Environmental Engineering, Anshun University, Anshun 561000, China; liuchao19890918@126.com

* Correspondence: pangli4286@163.com; Tel.: +86-130-3780-7271

Abstract: Calcium (Ca) is an essential plant nutrient and cell signal element, but in the cultivation of container seedlings, the regulatory effect of Ca on seedling nitrogen nutrition and its regulatory mechanism have been neglected. Ectomycorrhizal fungi (ECMF) inoculation is widely used in forest container seedling cultivation. Thus, we added a certain amount of Ca to the culture matrix to determine how the cooperation between Ca and ECMF improves the nitrogen nutrition of *Pinus massoniana* ectomycorrhizal (ECM) container seedlings. We found that addition Ca significantly increased the relative abundance of *Actinomycetota* and *Bacillota* in the rhizosphere of ECM seedlings. These enriched bacteria cooperated with the ECMF and significantly enhanced extracellular enzyme NAG and LAP secretion. Meanwhile, adding Ca promoted the microbial nitrogen cycle in the ECM seedlings rhizosphere, and the relative abundances of nitrogen fixation genes (*nifD*, *nifH*, *nifK*) and the dissimilatory nitrate reduction gene (*narH*) significantly increased. In addition, Ca promoted the infection of ECMF on seedlings and induced the sprouting of absorptive roots with larger diameter ($0.5 \text{ mm} < RD \leq 2.0 \text{ mm}$), i.e., ECM seedlings adopted a dual strategy of enhancing mycorrhizal symbiosis and improving root absorption area to obtain soil nitrogen. These effects contributed to an increase in microbial biomass nitrogen (MBN) and seedling nitrogen content by 20.65% and 54.38%, respectively. The results provide an effective method and theoretical reference for improving the quality of container seedlings and increasing the ECM plantations early productivity.

Keywords: calcium; mycorrhizal container seedlings; microbial community composition; plant nitrogen nutrition; rhizosphere nitrogen cycling

Citation: Pang, L.; Wang, Y.; Qiao, Z.; Zhou, W.; Liu, C. Effect of Calcium and Ectomycorrhiza Collaboration on Nitrogen Nutrition and Rhizosphere Microbial Community of *Pinus massoniana* L. Container Seedlings. *Forests* **2024**, *15*, 2068. <https://doi.org/10.3390/f15122068>

Academic Editor: Adele Muscolo

Received: 23 October 2024

Revised: 13 November 2024

Accepted: 19 November 2024

Published: 22 November 2024



Copyright: © 2024 by the authors. Submitted for possible open access publication under the terms and conditions of the Creative Commons Attribution (CC BY) license (<https://creativecommons.org/licenses/by/4.0/>).

1. Introduction

Nitrogen (N), an essential macronutrient for plant growth and development, plays an irreplaceable role in plant organ construction, material metabolism, and productivity formation [1]. In forest ecosystems, ectomycorrhizal fungi (ECMF) commonly form ectomycorrhizae with tree roots [2], which help host plants efficiently acquire N nutrients [3–5]. In exchange, plants excrete photosynthetic fixed carbon-containing organic matter to the rhizosphere, which strongly affects the root circumference microecosystem [6]. Therefore, ectomycorrhizal inoculation is very valued in seedling raising and afforestation. However, nutrient exchange and stable symbiosis between host plants and mycorrhizal fungi are regulated by plant nutrition status and soil physicochemical properties [2].

Calcium (Ca) is one of the essential nutrients for plant growth and development [7]. As a cell signaling molecule, Ca is a major plant cell metabolism regulator [8,9]. Adding calcium fertilizer to the soil can promote plant growth and improve plant quality [10]. Under salt [11,12], drought [13], acid rain [14], and heavy metals [15] stress, Ca can enhance plant resilience [16]. Additionally, Ca can improve the physical and chemical properties of soil, increase the agglomeration of soil, and play a good role in regulating soil microgrowth. Moreover, Ca encourages plants to establish symbiotic relationships with microorganisms (rhizobia, arbuscular mycorrhizal fungi) [17,18]. For example, calcium fertilizer application can improve the interaction between peanut roots and rhizobia, and improve peanut symbiosis N fixation efficiency [19].

Adding a certain amount of Ca to the soil helps soil microorganisms convert plant litter into persistent soil organic matter, thereby increasing soil organic carbon (SOC) storage [20]. The biological mechanism triggered by Ca increases hyphae-forming bacteria abundance, which then regulates plant litter decomposition and promotes litter proportion transformation into microbial biomass [20]. Therefore, calcium has a beneficial effect on the soil organic carbon cycle. However, the soil carbon and nitrogen cycles are the most closely linked [21,22], and Ca impacts on ectomycorrhizal symbiosis, rhizosphere microbial community structure, and seedling nitrogen nutrition remain unclear.

Pinus massoniana, a widely distributed fast-growing timber tree, is a typical ectomycorrhizal tree species. The addition of an appropriate amount of calcium to the soil markedly improves *Pinus massoniana* seedlings growth and development [23,24]. The rhizosphere is a hotspot for root nutrient absorption, litter deposition, microbial activity, and plant–matrix–microbe interactions [25,26]. Given the significant regulatory effects of exogenous Ca on soil microbial communities and the carbon cycle, we investigated the impact of Ca addition on *Pinus massoniana* mycorrhizal container seedlings nitrogen nutrition and rhizosphere nitrogen cycling, using metagenomic sequencing to reveal interactions with rhizosphere microorganisms. This study is helpful to understanding the mechanism of calcium on forest-ECMF high efficient symbiosis, and provides a reference for using calcium to improve seedling productivity of ECM plantation.

2. Materials and Methods

2.1. Experimental Site and Materials

The experiment was conducted in a greenhouse at Anshun University, Guizhou Province (26.16° N, 106.98° E), at 1410 m elevation. This location has a subtropical humid monsoon climate with an average annual temperature of 14 °C, annual rainfall of 1188.5 mm, and a frost-free period of 267–282 days. The experimental material was an excellent progeny from a second-generation *Pinus massoniana* breeding population of controlled cross-pollinated 6627 (Jiangxi) × 5907 (Zhejiang), provided by the Key Laboratory for Subtropical Forestry Cultivation of the State Forestry and Grassland Administration (Hangzhou, China). The ECMF used was *Pisolithus tinctorius* (Pers.) Coker & Couch strain cfc7668, purchased from the China General Microbiological Culture Collection Center (Beijing, China). Peat, perlite, and vermiculite were mixed at a volumetric ratio of 5:2:1, and placed in a high-temperature and high-pressure sterilizer at 121 °C for 2 h. After cooling, they were loaded into plastic pots with a top diameter of 12 cm and a height of 15 cm. The pH 7.2 culture matrix contained total nitrogen (0.91 g/kg), total phosphorus (0.22 g/kg), total potassium (5.56 g/kg), available nitrogen (84.90 mg/kg), available phosphorus (1.66 mg/kg), available potassium (62.38 mg/kg), exchangeable Ca (11.55 cmol/kg), and organic matter (62.15 g/kg).

2.2. Experimental Setup

The experiment included four treatments: control (CK group), ECMF inoculation (ECMF group), 20 mmol/L CaCl₂ addition (Ca group), and ECMF inoculation + 20 mmol/L CaCl₂ (EC group). The CaCl₂ concentration was determined through a preliminary

experiment, with set concentrations of 0, 10, 20, 30, and 40 mmol/L, where 20 mmol/L CaCl_2 had the most significant impact on seedling growth after 4 months of cultivation. The experiment was a completely randomized block design, with single plant plots and six blocks (to mitigate environmental influences on the experiment), meaning each treatment had six replicates (Figure 1).

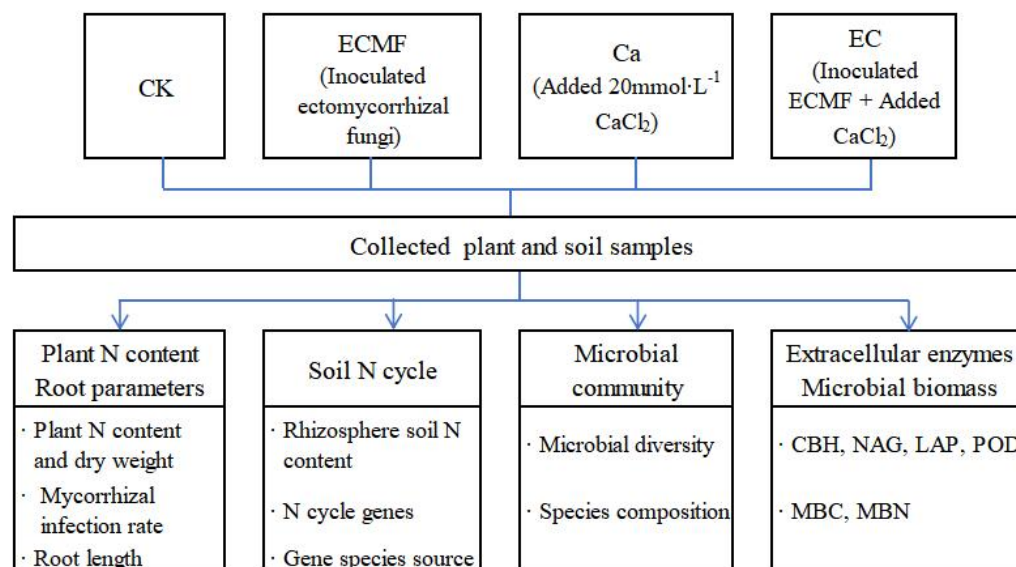


Figure 1. Experimental design. CBH: cellobiohydrolase, NAG: N-acetyl- β -D-glucosidase, LAP: leucine aminopeptidase, POD: peroxidase, MBC: microbial biomass carbon, MBN: microbial biomass nitrogen.

Pinus massoniana seeds were sterilized by soaking in 0.4% KMnO_4 solution for 20 min, rinsed several times with sterile water, and then placed on sterilized wet filter paper in a petri dish. The seeds were germinated in an artificial climate chamber at 25 °C for 5–7 days. Once the seeds showed a white tip, the sowing experiment commenced. Sowing took place in early March 2023. During sowing, the ECMF group and EC group had 0.3 g of *Pisolithus tinctorius* (Pers.). Coker & Couch fungal fertilizer was added below the sowing holes, while the CK group and Ca group received the same amount of sterilized fungal fertilizer. Then, 2–3 seeds were sown in each hole and covered with 2 cm of growing medium. After emergence, seedlings with uniform growth were selected from each treatment, retaining one plant per pot. After three months post-planting, once ectomycorrhiza had formed, Ca addition experiments were initiated. A 200 mL solution of 20 mmol/L CaCl_2 was uniformly sprayed on the seedling root zone in the Ca and EC groups, while the CK and ECMF groups received an equal volume of distilled water. These applications were repeated every 7 days for two months. During the experiment, pot soil moisture was maintained between 70–80% to meet *Pinus massoniana* seedling normal water requirements. Seedlings were harvested in early October 2023, 7 months after sowing. The collected rhizosphere soil samples were loaded into 20 mL EP tubes and stored at -70 °C for metagenomic analysis.

2.3. Test Methods

2.3.1. Plant Traits and Soil Nitrogen Content Determination

The harvested seedlings were thoroughly washed with distilled water and divided into roots and shoots. An EPSON (Suwa, Japan) perfection V700 scanner was used to scan all the roots, obtaining root scan images for each group. These images were analyzed using WinRHIZO Pro 2016 software (Regent Instruments Inc., Quebec City, QC, Canada) for morphological parameters of the root system, including total root length (RL) and lengths

of absorptive roots in various diameter classes ($0 \text{ mm} < \text{root diameter } [RD] \leq 0.5 \text{ mm}$, $0.5 \text{ mm} < RD \leq 2.0 \text{ mm}$), as well as root surface area.

Thirty 1–2 cm root segments were randomly selected from each treatment (4 repetitions), mycorrhizal morphology was observed, and fungal infection was counted using a TSD6745 stereomicroscope (Suzhou Sadie Precision Instrument Co., Ltd., Suzhou, China). Mycorrhizal infection ratio (*MIR*) = infected root tips/total root tips selected $\times 100\%$ [27], calculating the average of 4 replicates.

Whole seedling samples were first blanched at $105 \text{ }^\circ\text{C}$ for 30 min and then dried at $60 \text{ }^\circ\text{C}$ to a constant weight to obtain the total dry weight. A suitable amount of dried, crushed plant material was digested with $\text{H}_2\text{SO}_4\text{-H}_2\text{O}_2$ and total nitrogen content was determined using the Kjeldahl method. Soil total nitrogen (*STN*) and alkali-hydrolyzable nitrogen (*SAN*) were measured using the Kjeldahl and alkaline diffusion methods, respectively.

2.3.2. Determination of Soil Extracellular Enzyme Activities and Microbial Biomass Carbon and Nitrogen

The activities of soil cellobiohydrolase (CBH), leucine aminopeptidase (S-LAP), N-acetyl- β -D-glucosidase (S-NAG), and peroxidase (S-POD) were measured according to the manufacturer's instructions provided by Sinobestbio Co. Ltd., China. Microbial biomass carbon (*MBC*) was determined using CHCl_3 fumigation- K_2SO_4 extraction, the extract carbon content was determined by an organic carbon analyzer, microbial biomass nitrogen (*MBN*) was determined using CHCl_3 fumigation- K_2SO_4 extraction, and the extract nitrogen content was determined by the Kjeldahl method [28].

2.3.3. Soil Metagenomic Sequencing and Data Analysis

1. Microbial community metagenomic sequencing

Total genomic DNA was extracted from each soil sample using the CTAB method [29]. Extracted DNA quality was tested using an Agilent 5400 (Agilent Technologies Co., Ltd., Palo Alto, CA, USA). An NEB Next[®] Ultra[™] II FS DNA Library Prep Kit (New England Biolabs, Ipswich, MA, USA) was used for library construction. Library yields were determined using an Agilent 2100 (Agilent Technologies Co. Ltd., Palo Alto, CA, USA). Library sequencing was conducted on the Illumina NovaSeq PE150 platform (San Diego, CA, USA) by Wekemo Tech Co., Ltd., Shenzhen, China.

2. Bioinformatics analysis

Raw data obtained from sequencing were quality-controlled (Trimmomatic, Version 0.39) and host-removed (Bowtie2, Version 2.3.5.1) using Kneaddata software (0.7.4). Quality control effectiveness was assessed using FastQC (Version 0.11.9) [30]. Clean sequencing data were annotated and classified with Kraken2. Species annotation resolution was evaluated across seven taxonomical levels (from kingdom to species). The higher the proportion of sequences at the species or genera level relative to the total number of sequences, the better the annotation performance of the samples. Bracken was then used to estimate the relative abundance of each sample.

Clean sample sequences were compared with the protein database (UNIREF90) using DIAMOND software (Version 0.8.22). To obtain gene functional annotations and relative abundances at various functional levels, the gene sequence Uniref90 IDs were matched against the Kyoto Encyclopedia of Genes and Genomes (KEGG) database. Based on the gene functional abundance table, a nitrogen cycle pathway map was constructed.

2.3.4. Data Statistical Analysis

Multifactor analysis of variance was conducted using IBM SPSS Statistics 19.0 software, and the Duncan test was used for multiple comparisons ($\alpha = 0.05$). Data visualization was performed using Origin Pro 2022 software. α -Diversity analysis was completed using Wekemo Bioincloud (<https://www.bioincloud.tech>, 16 August 2024), and significant differences between groups were considered at $p < 0.05$. To identify the

dominant species within microbial communities in Ca addition treatments, biomarkers with significant differences were defined by LEfSe analysis ($LDA > 2$). To evaluate the direct and indirect associations of nitrogen cycle genes, microbial biomass, extracellular enzymes, and root parameters with plant nitrogen content, a structural equation model (SEM) was constructed using IBM SPSS Amos 25.0 software. The relative importance of major variables in predicting plant nitrogen content was assessed using an RF model by Wekemo Bioincloud (<https://www.bioincloud.tech>, 20 August 2024).

3. Results and Analysis

3.1. Impact of Ca on ECM Seedling Rhizosphere Microbial Community Structure

Metagenomic analysis revealed that microbial community composition in the *Pinus massoniana* mycorrhizal seedling rhizosphere consisted of 99.41% bacteria, 0.44% fungi, and 0.14% archaea. Among these, phyla with higher relative abundance in fungi included *Ascomycota*, *Basidiomycota*, *Mucoromycota*, and *Cryptomycota*. Dominant bacterial phyla were *Pseudomonadota*, *Actinomycetota*, *Bacillota*, and *Verrucomicrobiota*, which collectively accounted for over 73% of total microbial rhizosphere abundance (Figure 2A). Ca addition significantly affected the microbial Chao1 index in the ECM seedling rhizosphere (Figure 2B). Non-metric multidimensional scaling (NMDS) analysis based on Bray–Curtis distances indicated that the CK and ECMF group, and the Ca and EC group formed two distinct microbial communities, showing significant separation along the first axis ($p < 0.001$) (Figure 2C). The latter significantly increased the relative abundance of *Actinomycetota* (orders *Micrococcales*, *Mycobacteriales*, *Propionibacteriales*, *Streptosporangiales*) and *Bacillota* (class *Bacilli*), while the relative abundance of the phylum *Pseudomonadota* decreased, although not significantly (Figures 2A and 3).

The Figure 2D Venn diagram shows the number of common and unique species within each group. LEfSe ($LDA > 2$) and cladogram analysis results (Figure 3) indicated that the EC group was significantly enriched in the largest number of differential species. At the family and genus levels, EC group was primarily enriched in bacteria with the potential to degrade organic nitrogen and fix inorganic nitrogen, such as *Streptomyetaceae*, *Arthrobacter*, *Mycolicibacterium*, *Pseudarthrobacter*, *Nocardiaceae*, *Rhodococcus*, *Gordonia*, *Nocardioides*, *Streptosporangiaceae*, *Xanthobacteraceae*, *Phyllobacterium*, *Mesorhizobium*, *Neorhizobium*, *Pseudomonadaceae*, *Bradyrhizobium*, and *Hyphomicrobiaceae*.

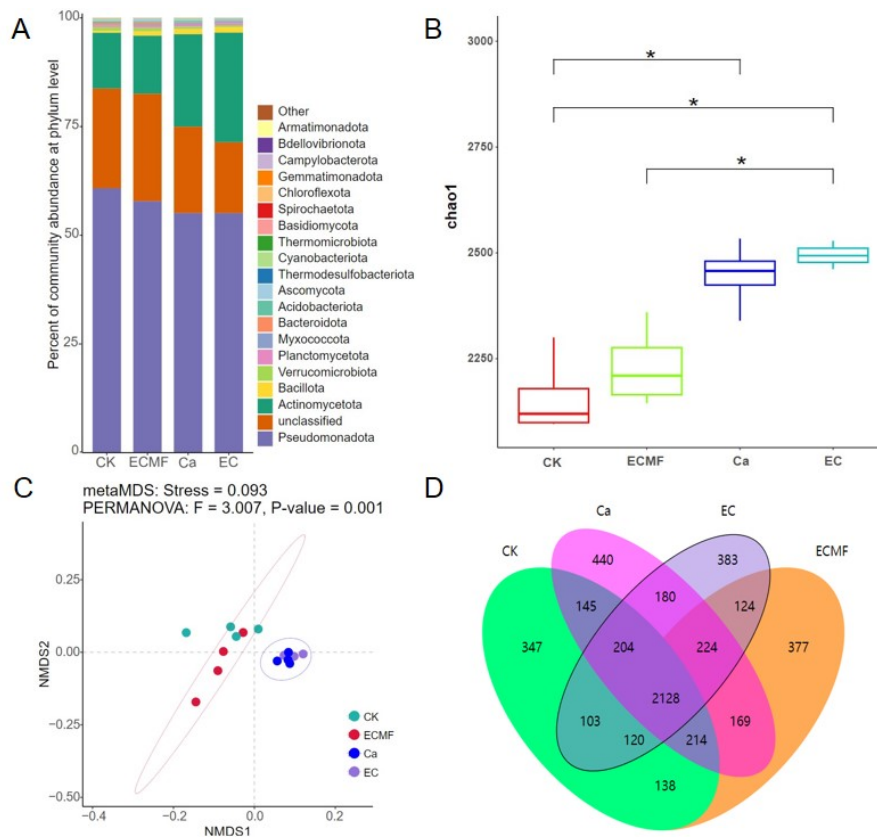
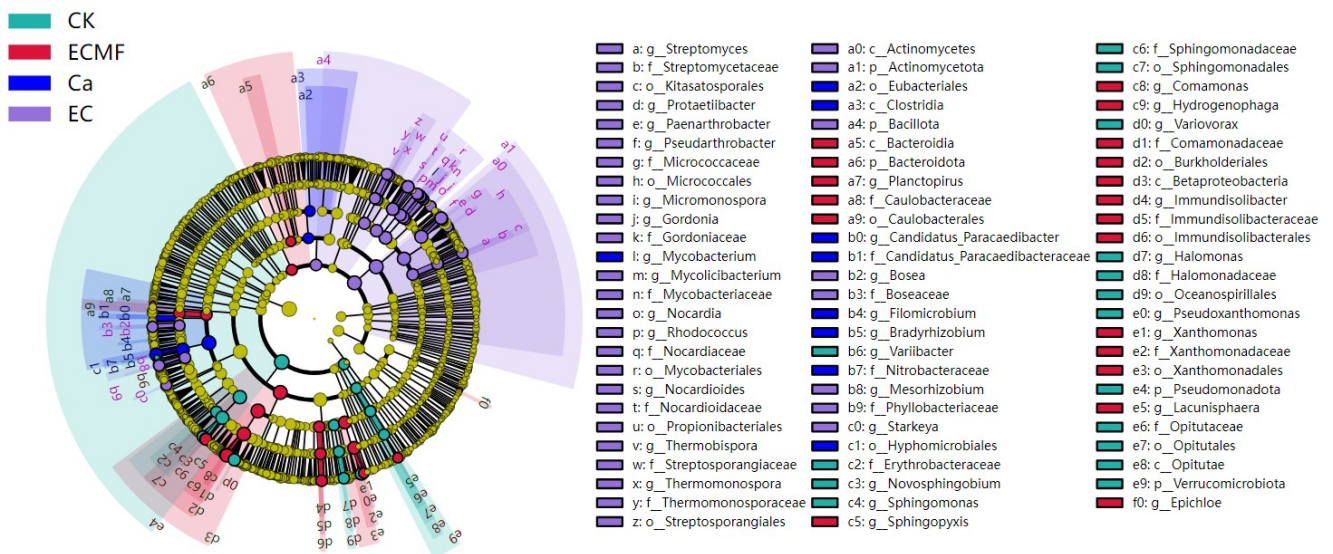


Figure 2. Effects of different treatments on soil bacterial communities. (A) Relative abundances of major bacterial phyla; (B) bacterial community Chao1 index; (C) NMDS map of bacterial communities based on Bray–Curtis distance; (D) Venn diagram of bacterial communities. * indicates that relative abundances are significant at $p < 0.05$.



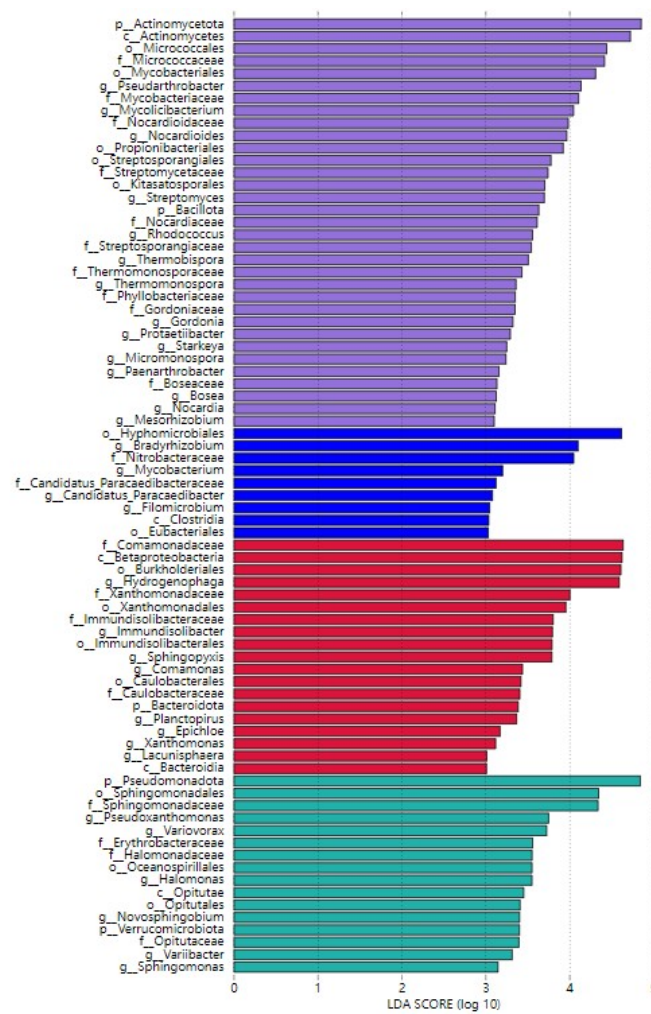


Figure 3. The cladogram illustrates species phylogenetic relationships in each group. Species differences between treatments and significantly different biomarkers between groups at the genus level (LDA default value 2.0).

3.2. Impact of Ca on Rhizosphere Microbial Biomass and Extracellular Enzyme Activity

MBC content in the rhizospheres of Ca and in EC groups was significantly higher than in the CK group, with increases of 10.09, 9.53, and 33.14%, respectively (Figure 4). Compared to the CK group, MBN content in the EC group increased significantly (by 20.65%). Clearly, Ca addition significantly enhanced EC group rhizosphere microorganism activity. Compared to the CK group, CBH, NAG, LAP, and POD activities in the EC group rhizosphere soil significantly increased, by 17.78, 11.62, 42.08, and 13.43%, respectively (Figure 5). CBH activity was in the order ECMF > EC > Ca > CK. CBH activity in the EC group was significantly reduced by 26.22% compared to the ECMF group. Thus, Ca addition did not significantly increase rhizosphere CBH activity.

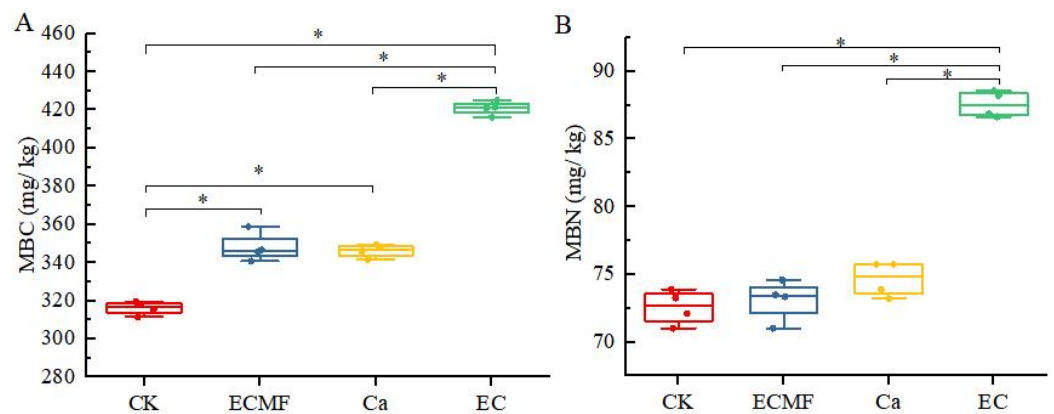


Figure 4. Differences in microbial biomass between treatments. (A,B) show the content of microbial biomass carbon (MBC) and microbial biomass nitrogen (MBN) under different treatments, respectively. *: $p < 0.05$.

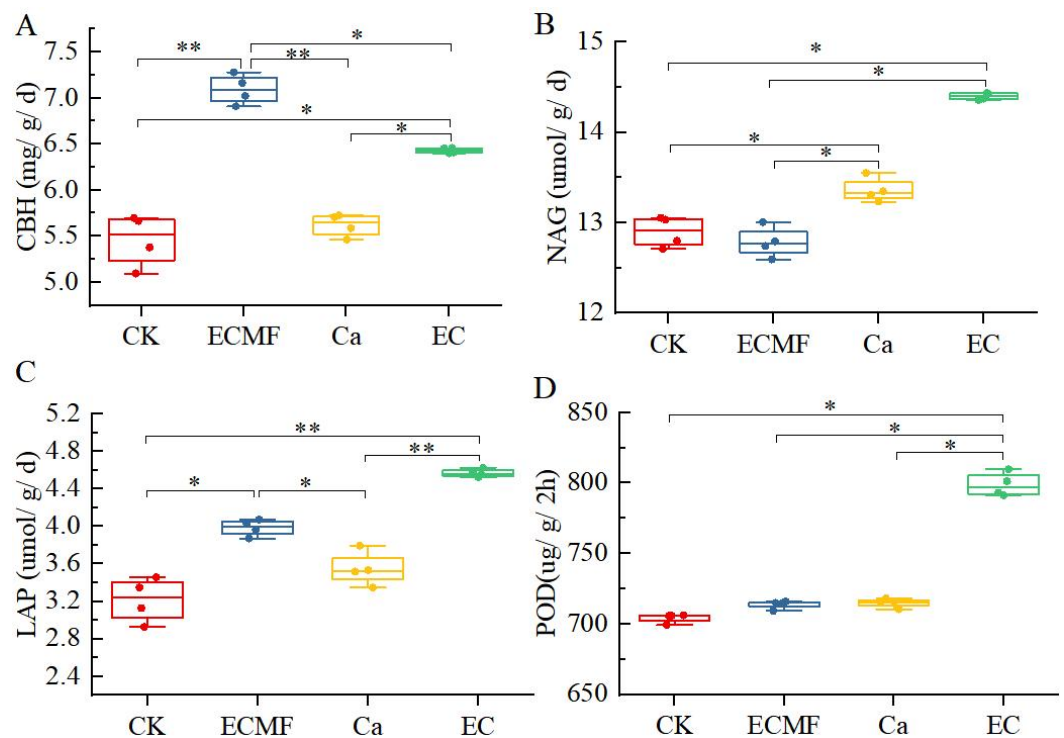


Figure 5. Differences in extracellular enzyme content between treatments. (A–D) are cellobiohydrolase (CBH), N-acetyl-β-D-glucosidase (NAG), leucine aminopeptidase (LAP), and peroxidase (POD) contents under different treatments, respectively. *: $p < 0.05$; **: $p < 0.01$.

3.3. Impact of Ca on Soil Nitrogen Cycling and Related Functional Genes Abundance

Soil nitrogen cycling pathway analysis revealed that in the EC group, both the nitrogen fixation and dissimilatory nitrate reduction pathways were significantly enhanced, while denitrification was reduced. Metagenomic sequencing analysis of genes involved in rhizosphere microbial nitrogen cycling identified 29 genes with relatively high abundances, of which 16 had clearly identified species origins. Compared to the CK group, the EC group showed significant increases in the relative abundances of nitrogen fixation genes *nifD*, *nifH*, and *nifK* and the dissimilatory nitrate reduction gene *narH* (Figure 6). The primary source species for these differential genes in the EC group were the phyla *Pseudomonadota* (genera *Immundisolibacter cernigliae*, *Hyphomicrobium sp MC1*, *Azotobacter beijerinckii*, *Azotobacter chroococcum*), and *Actinomycetota* (genera *Arthrobacter sp HMWF013*, *Intrasporangium calvum*).

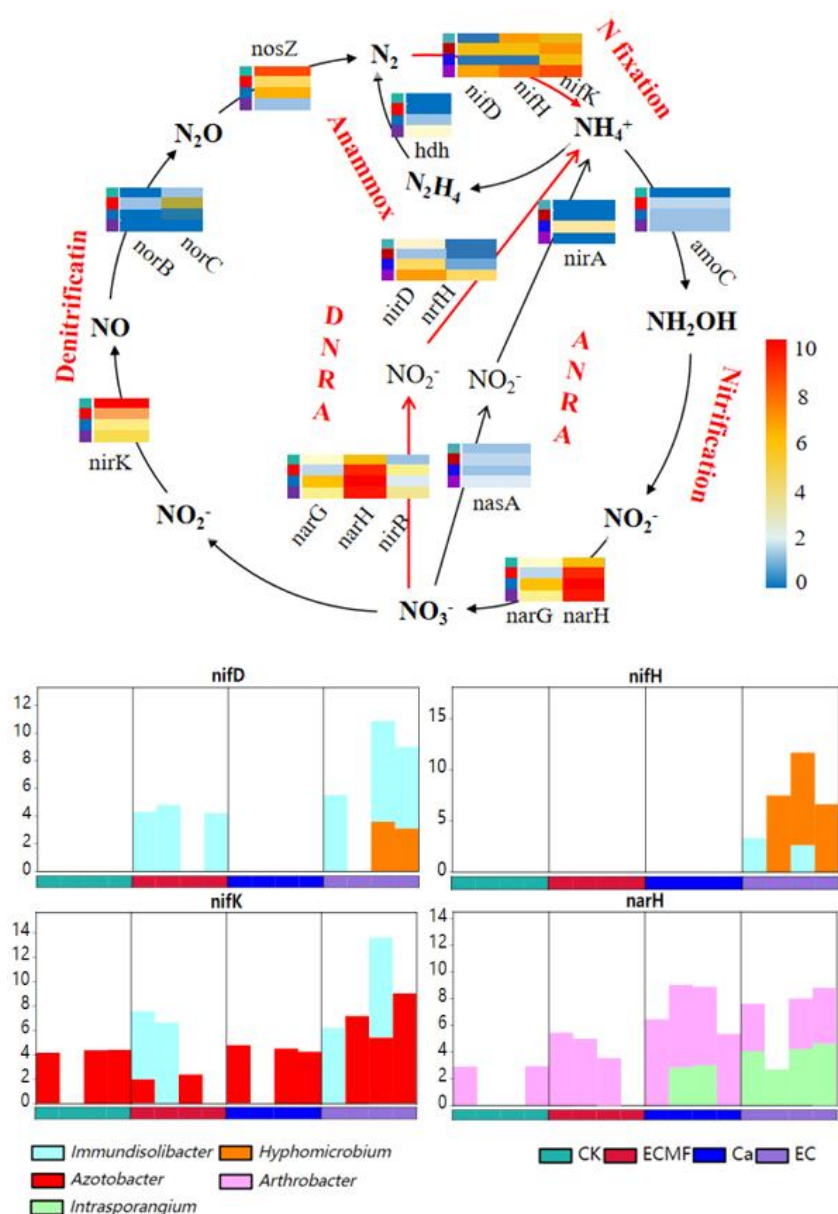


Figure 6. Relative abundance of major functional genes involved in nitrogen cycling and their species origins.

3.4. Impact of Ca on ECM Seedling Nitrogen Nutrition and Soil Nitrogen Content

Compared to the CK group, seedling total nitrogen content from the Ca and EC groups increased by 22.64 and 54.38%, respectively, and seedling dry weight was enhanced by 28.93 and 55.37% (Figure 7A,B). Nutrient content analysis in the rhizosphere soil indicated that total and available nitrogen content in the Ca and EC groups were significantly lower than in the CK and ECMF groups (Figure 7E,F). This suggests that Ca addition significantly improved root absorption efficiency and nitrogen utilization in the rhizosphere soil of ECM seedlings.

EC seedling mycorrhizal infection rate significantly increased (by 25.68%) compared with the ECMF group (Figure 7C), indicating that Ca promoted ECMF infection of seedling roots. Analysis of root parameters showed significant increases in total RL and surface area for the ECMF, Ca, and EC groups. Specifically, total RL increased by 1.24 times, 28.92%, and 1.01 times compared to the CK group, but surface area increased by 1.07 times, 32.89%, and 1.32 times, respectively (Figures 7D and 8B). From root system analysis, it was evident that the increase in FRL (fine root length) within the diameter

range of $0.5 \text{ mm} < RD \leq 2.0 \text{ mm}$ was greater than within the range of $0 \text{ mm} < RD \leq 0.5 \text{ mm}$ for EC groups. This may explain the larger increase in root surface area in the EC group. Root scanning revealed that lateral roots in the EC group were longer and more branched, suggesting that the root system may extend into larger soil spaces (Figure 8A).

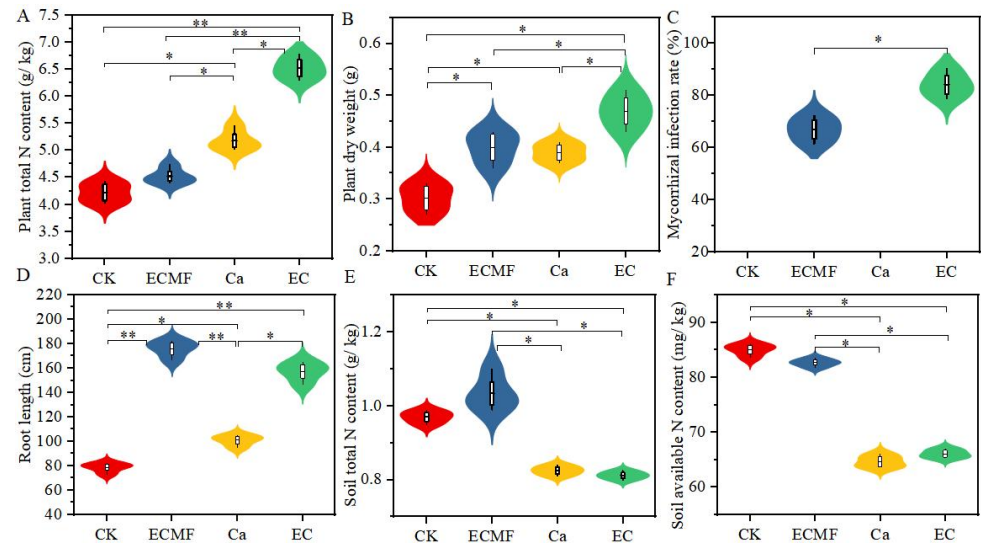


Figure 7. Differences in plant and soil nitrogen content and root parameters between treatments. *: $p < 0.05$; **: $p < 0.01$. (A–D) representing parameters related to plant nitrogen nutrition respectively; (E,F) representing the content of total nitrogen and available nitrogen of soil.

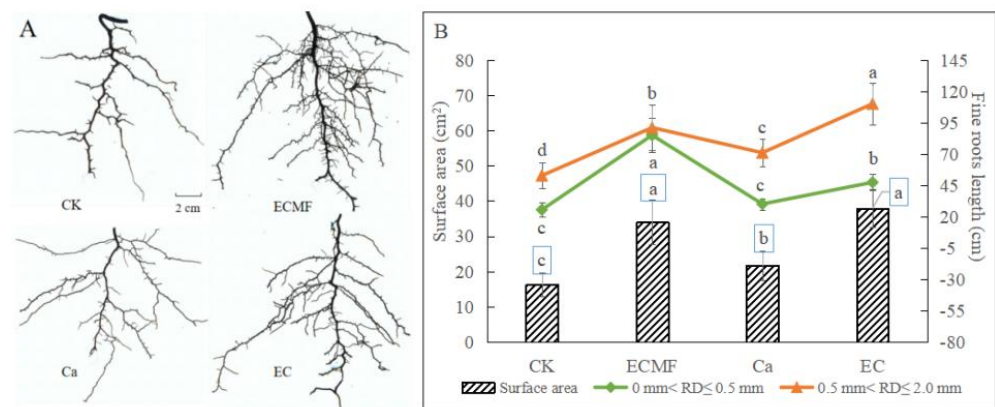


Figure 8. Root scanning images for each group, showing root surface area and FRL at different diameter ranges. (A) root scanning images; (B) root surface area, a total of $0 \text{ mm} < \text{root diameter } [RD] \leq 0.5 \text{ mm}$ and $0.5 \text{ mm} < RD \leq 2.0 \text{ mm}$ fine roots within different diameter ranges. Different lowercase letters indicate significant differences between groups at $p < 0.05$.

3.5. SEM and RF Analysis of the Main Factors Affecting Seedling Nitrogen Content

According to the SEM model, microbial biomass (MBC, MBN), extracellular enzyme activities (CBH, NAG, LAP, POD), and root parameters (MIR, RL, FRL) all significantly influenced seedling total nitrogen content, with path coefficients of 0.76, 0.50, and 0.54, respectively (Figure 9). The direct impact of nitrogen cycle-related genes (*nifD*, *nifH*, *nifK*, *narH*) on seedling total nitrogen content was not significant; however, their interactions with extracellular enzyme activities and microbial biomass were significant, with path coefficients of 0.74 and 0.51. This indicates that nitrogen cycling genes indirectly affect seedling total nitrogen content by regulating extracellular enzyme activities and microbial biomass. RF analysis explored the relative importance of different variables on seedling nitrogen content. In the EC group, the nitrogen fixation genes *nifD*, *nifK*, and the

extracellular enzyme NAG had significant predictive power for seedling nitrogen absorption and utilization (nitrogen content) (Figure 10).

$$\chi^2 = 688.21, \text{CMIN/DF} = 3.529, \text{GFI} = 0.972, \text{NFI} = 0.966, \text{RMSEA} = 0.057 \quad (1)$$

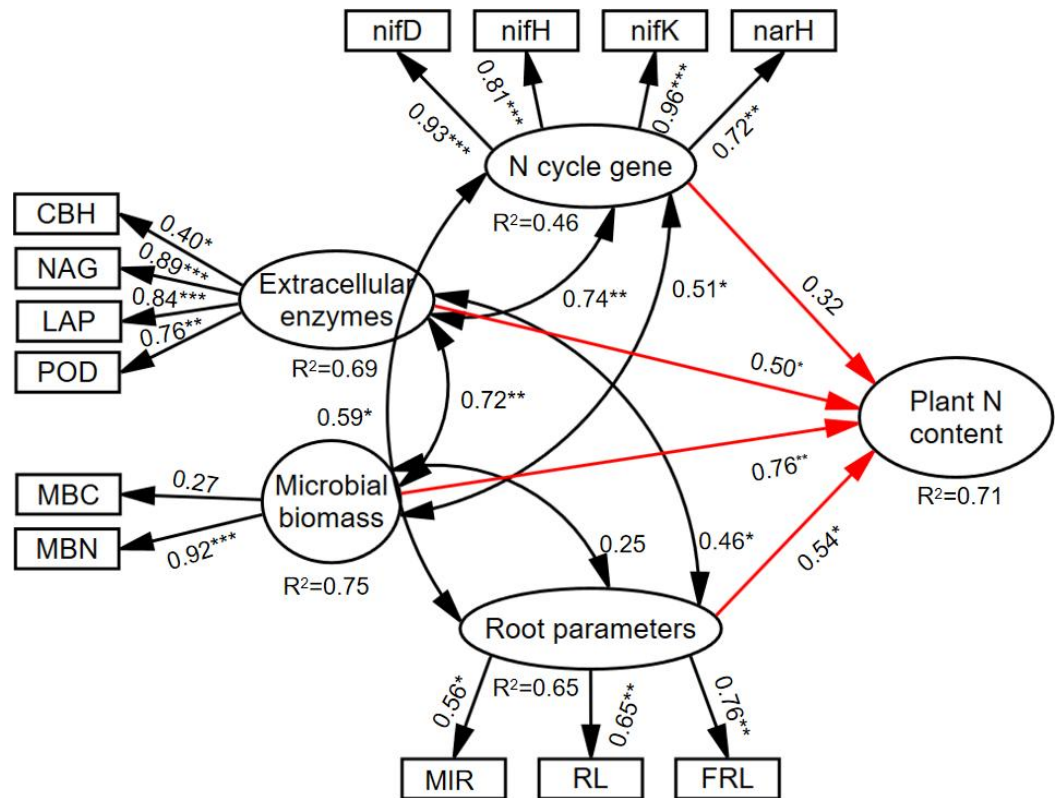


Figure 9. SEM model of the main factors affecting seedling nitrogen content. Red arrows represent the latent variable affecting seedling nitrogen content. *MIR*: mycorrhizal infection rate, *RL*: total roots length, *FRL*: 0.5 mm < root diameter [RD] ≤ 2.0 mm absorptive roots length. Numbers on the lines represent standardized path coefficients, and the R² values indicate the proportion of variance explained. *, **, *** indicate significance of variables at $p < 0.05$, $p < 0.01$, $p < 0.001$, respectively.

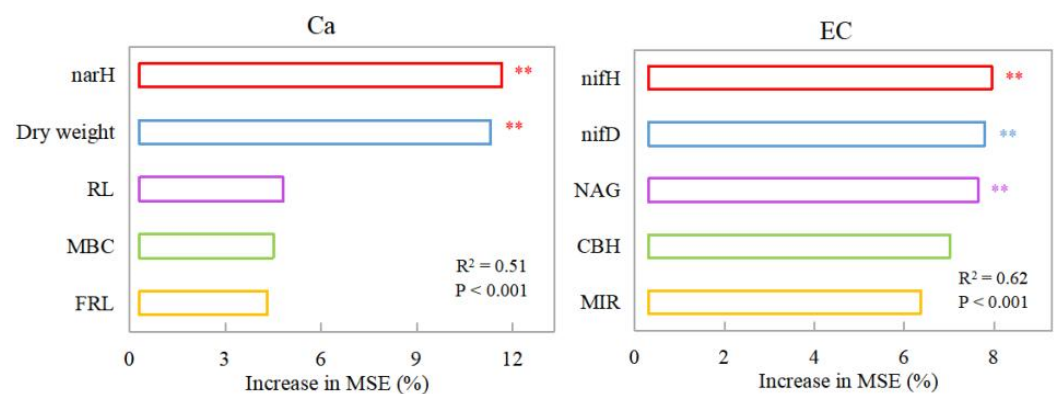


Figure 10. RF analysis results showing the relative importance of the main variables in predicting seedling nitrogen content. R² values indicate the proportion of variance explained, $p < 0.001$ indicates the significance of the model. MSE, mean square error, where higher values imply greater importance of the variable, ** indicates significance at $p < 0.01$.

4. Discussion

4.1. Calcium Altered the Microbial Community Composition in Container Seedling Rhizosphere

In this study, metagenomic analysis showed that Ca significantly increased the relative abundance of *Actinomycetota* and *Bacillota* in the mycorrhizal container seedling rhizosphere. Enriched bacteria such as *Streptomyetaceae*, *Arthrobacter*, *Mycolicibacterium*, *Pseudarthrobacter*, *Nocardiaceae*, *Rhodococcus*, *Xanthobacteraceae*, *Bradyrhizobium*, and *Hyphomicrobiaceae* could potentially degrade organic nitrogen and fix inorganic nitrogen. Shabtai [11] showed that exogenous Ca promoted the enrichment of *Bacillota* (class *Bacilli*) and *Actinomycetota* (classes *Actinomycetes* and *Thermoleophilia*) as well as some *Pseudomonadota* members. Our results were similar, but the number of specific bacteria in the ECM seedling rhizosphere after Ca addition was significantly higher than in the seedling roots without ECMF colonization (Ca group). This shows that Ca can regulate rhizosphere bacteria and ECMF interactions, increasing the enrichment of specific bacteria. The following reasons may explain why Ca affected ECM seedling rhizosphere microbial community composition. As a general plant cell metabolism regulator, Ca can regulate the light signaling pathway [31] and photosynthetic organ function [32], thus improving ECM seedling photosynthetic efficiency. Therefore, plants have more photosynthetic carbon products to distribute to the rhizosphere as root exudates, thus providing a large carbon source for fungal and bacterial growth. Notably, up to half of the carbon fixed by photosynthesis is transferred to roots and their symbiotic fungi [33]. Rich carbon sources tend to form thriving rhizosphere microbial communities [34]. Additionally, root exudate type is also a key factor causing rhizosphere bacterial colonization [35,36]. Ca may also regulate root exudate composition, inducing these enriched bacteria to colonize in the rhizosphere. Further research is needed to confirm this hypothesis.

4.2. Ca Increased the Rhizosphere Nitrogen Cycle and Plant Nitrogen Content of Container Seedling

Changes in microbial community structure will inevitably affect soil nutrient cycling [37]. In this study, we found that Ca addition enhanced the nitrogen fixation and dissimilatory nitrate reduction pathways, while the relative abundances of nitrogen fixation genes (*nifD*, *nifH*, *nifK*) and the dissimilatory nitrate reduction gene (*narH*) significantly increased. Nitrogen cycling genes regulated rhizosphere extracellular enzyme secretion and microbiological activity to fix inorganic nitrogen and degrade organic nitrogen. Therefore, MBN and seedling nitrogen content increased by 20.65% and 54.38%, respectively. We found that the major source species of these genes were in *Actinomycetota* and *Pseudomonadota*. Adding Ca significantly increased *Actinomycetota* relative abundance in the ECM seedling rhizosphere. Thus, these results suggest that Ca promoted ECMF and enriched bacteria collaboration to increase NAG and LAP secretion. Meeds [38] showed that some rhizosphere bacteria could interact with ECMF to affect soil nutrient cycling and plant nutrient uptake. For example, ECMF and bacteria collaborate to increase the secretion of extracellular enzymes to promote soil nitrogen activation [4]. Extracellular enzymes play an important role in promoting soil organic matter decomposition and nutrient mineralization [39,40]. Additionally, we found that compared with the nitrogen acquiring enzyme, carbon acquiring enzyme CBH activity did not increase significantly after Ca addition. Although Ca addition reduced the degradation of soil organic carbon catalyzed by CBH, MBC increased significantly. This part of the carbon component may originate from the host plant.

4.3. Ca Altered the Acquisition Strategy of Mycorrhizal Container Seedling for Soil Nitrogen

Mycorrhizal symbiosis, which can extend the range of nutrient uptake by roots, is an important way for trees to acquire nutrient resources in barren environments [41,42]. Ca promoted ECMF infection roots to increase nitrogen absorption by container seedlings.

When Ca regulates plant metabolism and promotes seedling growth, it increases the nutrient requirement and forces roots to form a closer symbiotic relationship with ECMF, so the seedling mycorrhizal infection rate increases. Moreover, Ca induced the sprouting of larger diameter absorptive roots to increase root absorption area. Meanwhile, seedling lateral roots tended to be longer and more branched, which may promote ECM seedling roots to expand into larger soil spaces. We suggested that ECM seedlings with Ca addition adopt a dual strategy of enhancing mycorrhizal symbiosis and changing root architecture to obtain soil nitrogen. Root evolution generally tends to reduce dependence on symbiotic fungi, while strengthening the direction of investment in root system resource acquisition and self-defense [43–46]. The effect of Ca on root nitrogen acquisition strategies of mycorrhizal container seedling needs to be further studied over the long term.

5. Conclusions and Significance

We showed that Ca addition altered the rhizosphere microbial community structure of *Pinus massoniana* mycorrhizal container seedlings, significantly increasing *Actinomycetota* and *Bacillota*'s relative abundance. These enriched bacteria cooperated with ectomycorrhizal fungi, raising the ECM seedling nitrogen content and dry weight by increasing extracellular enzyme activity and microbial biomass. Therefore, our results are helpful to understand the effects of Ca on the rhizosphere microbial community, and provide an effective way to improve the nitrogen content of mycorrhizal container seedlings.

Author Contributions: L.P. and Y.W. designed the experiment. L.P. and W.Z. analyzed the data. L.P., Z.Q., W.Z., and C.L. reviewed and checked all the details. L.P. wrote the paper. All authors have read and agreed to the published version of the manuscript. All authors have read and agreed to the published version of the manuscript.

Funding: This work was supported by the Science and Technology Top Talent Project of Guizhou [grant number QianJiaoHeKY [2020]040]; the Agricultural Science and Technology Plan Project of Anshun [grant number [2022]01]; and the Science and Technology Program of Guizhou [grant number QianKeHeLH [2014]7497]. The funders had no role in study design, data collection and analysis, decision to publish, or preparation of the manuscript.

Data Availability Statement: The original contributions presented in the study are included in the article; further inquiries can be directed to the corresponding author.

Conflicts of Interest: The authors declare no conflicts of interest.

References

1. Xu, G.; Fan, X.; Miller, A. Plant nitrogen assimilation and use efficiency. *Annu. Rev. Plant Biol.* **2012**, *63*, 153–182. <https://doi.org/10.1146/annurev-arplant-042811-105532>.
2. Yu, J.; Yuan, H. Research progress on symbiotic interaction and host selection mechanisms of ectomycorrhizal fungi. *Mycosystema* **2023**, *42*, 86–100. <https://doi.org/10.13346/j.mycosystema.220360>.
3. Shi, J.; Wang, X.; Wang, E. Mycorrhizal symbiosis in plant growth and stress adaptation: From genes to ecosystems. *Annu. Rev. Plant Biol.* **2023**, *74*, 569–607. <https://doi.org/10.1146/annurev-arplant-061722-090342>.
4. Cheeke, T.E.; Phillips, R.P.; Brzostek, E.R.; Rosling, A.; Bever, J.D.; Fransson, P. Dominant mycorrhizal association of trees alters carbon and nutrient cycling by selecting for microbial groups with distinct enzyme function. *New Phytol.* **2017**, *214*, 432–442. <https://doi.org/10.1111/nph.14343>.
5. Deng, M.; Hu, S.; Guo, L.; Jiang, L.; Huang, Y.; Schmid, B.; Liu, C.; Chang, P.; Li, S.; Liu, X. Tree mycorrhizal association types control biodiversity-productivity relationship in a subtropical forest. *Sci. Adv.* **2023**, *9*, eadd4468. <https://doi.org/10.1126/sciadv.add4468>.
6. Duan, S.; Feng, G.; Limpens, E.; Bonfante, P.; Xie, X.; Zhang, L. Cross-kingdom nutrient exchange in the plant-arbuscular mycorrhizal fungus-bacterium continuum. *Nat. Rev. Microbiol.* **2024**, *22*, 773–790. <https://doi.org/10.1038/s41579-024-01073-7>.
7. White, P.J.; Broadley, M.R. Calcium in plants. *Ann. Bot.* **2003**, *92*, 487–511. <https://doi.org/10.1093/aob/mcg164>.
8. Kudla, J.; Becker, D.; Grill, E.; Hedrich, R.; Hippler, M.; Kummer, U.; Parniske, M.; Romeis, T.; Schumacher, K. Advances and current challenges in calcium signaling. *New Phytol.* **2018**, *218*, 414–431. <https://doi.org/10.1111/nph.14966>.
9. Feng, D.; Wang, X.; Gao, J.; Zhang, C.; Liu, H.; Liu, P.; Sun, X. Exogenous calcium: Its mechanisms and research advances involved in plant stress tolerance. *Front. Plant Sci.* **2023**, *14*, 1143963. <https://doi.org/10.3389/fpls.2023.1143963>.

10. Ma, H.; Wang, S.; Zhou, Y. Research progress of calcium-dependent protein kinases in plants. *J. Nanjing Agric. Univ.* **2017**, *40*, 565–572.
11. Roy, P.R.; Tahjib-Ul-Arif, M.; Polash, M.A.S.; Hossen, M.Z.; Hossain, M.A. Physiological mechanisms of exogenous calcium on alleviating salinity-induced stress in rice (*Oryza sativa* L.). *Physiol. Mol. Biol. Plants* **2019**, *25*, 611–624. <https://doi.org/10.1007/s12298-019-00654-8>.
12. Guo, Y.; Liu, Y.; Zhang, Y.; Liu, J.; Gul, Z.; Guo, X.-R.; Abozeid, A.; Tang, Z.-H. Effects of exogenous calcium on adaptive growth, photosynthesis, ion homeostasis and phenolics of *Gleditsia sinensis* Lam. plants under salt stress. *Agriculture* **2021**, *11*, 978. <https://doi.org/10.3390/agriculture11100978>.
13. Hu, W.; Tian, S.B.; Di, Q.; Duan, S.H.; Dai, K. Effects of exogenous calcium on mesophyll cell ultrastructure, gas exchange, and photosystem II in tobacco (*Nicotiana tabacum* Linn.) under drought stress. *Photosynthetica* **2018**, *56*, 1204–1211. <https://doi.org/10.1007/s11099-018-0822-8>.
14. Liu, T.W.; Wu, F.H.; Wang, W.H.; Chen, J.; Li, Z.J.; Dong, X.J.; Patton, J.; Pei, Z.M.; Zheng, H.L. Effects of calcium on seed germination, seedling growth and photosynthesis of six forest tree species under simulated acid rain. *Tree Physiol.* **2011**, *31*, 402–413. <https://doi.org/10.1093/treephys/tpr019>.
15. Jiang, S.; Liu, Y.; Shu, Y. Biochar and exogenous calcium assisted alleviation of Pb phytotoxicity in water spinach (*Ipomoea aquatica* Forsk) cultivated in Pb-spiked soil. *Environ. Geochem. Health* **2022**, *44*, 207–219. <https://doi.org/10.1007/s10653-021-00977-0>.
16. Shabbir, R.; Javed, T.; Hussain, S.; Ahmar, S.; Naz, M.; Zafar, H.; Pandey, S.; Chauhan, J.; Siddiqui, M.H.; Pinghua, C. Calcium homeostasis and potential roles in combatting environmental stresses in plants. *S. Afr. J. Bot.* **2022**, *148*, 683–693. <https://doi.org/10.1016/j.sajb.2022.05.038>.
17. Del Cerro, P.; Cook, N.M.; Huisman, R.; Dangeville, P.; Grubb, L.E.; Marchal, C.; Ho Ching Lam, A.; Charpentier, M. Engineered CaM2 modulates nuclear calcium oscillation and enhances legume root nodule symbiosis. *Proc. Natl. Acad. Sci. USA* **2022**, *119*, e2200099119. <https://doi.org/10.1073/pnas.2200099119>.
18. Fu, W.; Yan, M.; Zhao, L.; Zeng, X.; Cai, B.; Qu, S.; Wang, S. Inoculation with arbuscular mycorrhizal fungi increase calcium uptake in *Malus robusta*. *Sci. Hortic.* **2023**, *321*, 112295. <https://doi.org/10.1111/nph.17077>.
19. Diao, R.; Yang, S.; Zhang, J.; Wang, J.; Peng, Z.; Yu, X.; Li, X.; Wan, S. The mechanisms of calcium regulation on peanut nodulation and nitrogen fixation analyzed by transcriptomes and metabolomics. *J. Peanut Sci.* **2022**, *51*, 1–7+17. <https://doi.org/10.14001/j.issn.1002-4093.2022.04.001>.
20. Shabtai, I.A.; Wilhelm, R.C.; Schweizer, S.A.; Höschen, C.; Buckley, D.H.; Lehmann, J. Calcium promotes persistent soil organic matter by altering microbial transformation of plant litter. *Nat. Commun.* **2023**, *14*, 6609. <https://doi.org/10.1038/s41467-023-42291-6>.
21. Zang, H.; Mehmood, I.; Kuzyakov, Y.; Jia, R.; Gui, H.; Blagodatskaya, E.; Xu, X.; Smith, P.; Chen, H.; Zeng, Z.; et al. Not all soil carbon is created equal: Labile and stable pools under nitrogen input. *Glob. Chang. Biol.* **2024**, *30*, e17405. <https://doi.org/10.1111/gcb.17405>.
22. Hu, Y.; Deng, Q.; Kätterer, T.; Olesen, J.E.; Ying, S.C.; Ochoa-Hueso, R.; Mueller, C.W.; Weintraub, M.N.; Chen, J. Depth-dependent responses of soil organic carbon under nitrogen deposition. *Glob. Chang. Biol.* **2024**, *30*, e17247. <https://doi.org/10.1111/gcb.17247>.
23. Hu, W.; Liu, J.; Liu, T.; Zhu, C.; Wu, F.; Jiang, C.; Wu, Q.; Chen, L.; Lu, H.; Shen, G.; et al. Exogenous calcium regulates the growth and development of *Pinus massoniana* detected by physiological, proteomic, and calcium-related genes expression analysis. *Plant Physiol. Biochem.* **2023**, *196*, 1122–1136. <https://doi.org/10.1016/j.plaphy.2023.03.009>.
24. Li, H.; Zhao, Y.; Weng, X.; Zhou, Y.; Zhang, S.; Liu, L.; Pei, J. The most suitable calcium concentration for growth varies among different tree species—Taking *Pinus tabuliformis*, *Pinus sylvestris* var. *mongolica*, *Populus*, and *Morus alba* as examples. *Forests* **2023**, *14*, 1437. <https://doi.org/10.3390/f14071437>.
25. Pathan, S.I.; Ceccherini, M.T.; Sunseri, F.; Lupini, A. Rhizosphere as hotspot for plant-soil-microbe interaction. In *Carbon and Nitrogen Cycling in Soil*; Datta, R., Meena, R.S., Pathan, S.I., Ceccherini, M.T., Eds.; Springer: Singapore, 2020; pp. 17–43.
26. Chepsergon, J.; Moleleki, L.N. Rhizosphere bacterial interactions and impact on plant health. *Curr. Opin. Microbiol.* **2023**, *73*, 102297. <https://doi.org/10.1016/j.mib.2023.102297>.
27. Chen, L.; Jiang, C.; Wang, X.; Feng, Q.; Liu, X.; Tang, Z.; Sun, O.J. Nutrient trade-offs mediated by ectomycorrhizal strategies in plants: Evidence from an *Abies* species in subalpine forests. *Ecol. Evol.* **2021**, *11*, 5281–5294. <https://doi.org/10.1002/ece3.7417>.
28. Gao, D.; Bai, E.; Wang, S.; Zong, S.; Liu, Z.; Fan, X.; Zhao, C.; Hagedorn, F. Three-dimensional map** of carbon, nitrogen, and phosphorus in soil microbial biomass and their stoichiometry at the global scale. *Glob. Change Biol.* **2022**, *28*, 6728–6740. <https://doi.org/10.1111/gcb.16374>.
29. Siegel, C.S.; Stevenson, F.O.; Zimmer, E.A. Evaluation and comparison of FTA card and CTAB DNA extraction methods for non-agricultural taxa. *Appl. Plant Sci.* **2017**, *5*, 1600109. <https://doi.org/10.3732/apps.1600109>.
30. Schmieder, R.; Edwards, R. Quality control and preprocessing of metagenomic datasets. *Bioinformatics* **2011**, *27*, 863–864. <https://doi.org/10.1093/bioinformatics/btr026>.
31. Zhao, Y.; Shi, H.; Pan, Y.; Lyu, M.; Yang, Z.; Kou, X.; Deng, X.W.; Zhong, S. Sensory circuitry controls cytosolic calcium-mediated phytochrome B phototransduction. *Cell* **2023**, *186*, 1230–1243.e1214. <https://doi.org/10.1016/j.cell.2023.02.011>.

32. Zhao, X.; Lin, S.; Yu, S.; Zhang, Y.; Su, L.; Geng, L.; Cheng, C.; Jiang, X. Exogenous calcium enhances the physiological status and photosynthetic capacity of rose under drought stress. *Hortic. Plant J.* **2024**, *10*, 853–865. <https://doi.org/10.1016/j.hpj.2023.01.010>.
33. Zhou, J.; Gube, M.; Holz, M.; Song, B.; Shan, I.; Shi, L.; Kuzyakov, Y.; Dippold, M.A.; Pausch, J. Ectomycorrhizal and non-mycorrhizal rhizosphere fungi increase root-derived C input to soil and modify enzyme activities: A ¹⁴C pulse labelling of *Picea abies* seedlings. *Plant Cell Environ.* **2022**, *45*, 3122–3133. <https://doi.org/10.1111/pce.14413>.
34. Wen, Z.; White, P.J.; Shen, J.; Lambers, H. Linking root exudation to belowground economic traits for resource acquisition. *New Phytol.* **2022**, *233*, 1620–1635. <https://doi.org/10.1111/nph.17854>.
35. Feng, H.; Fu, R.; Hou, X.; Lv, Y.; Zhang, N.; Liu, Y.; Xu, Z.; Miao, Y.; Krell, T.; Shen, Q.; et al. Chemotaxis of beneficial rhizobacteria to root exudates: The first step towards root-microbe rhizosphere interactions. *Int. J. Mol. Sci.* **2021**, *22*, 6655. <https://doi.org/10.3390/ijms22136655>.
36. Lin, H.; Lai, C.; Yu, G.; Sunahara, G.I.; Liu, L.; Ullah, H.; Liu, J. Root exudate-driven rhizospheric recruitment of plant growth-promoting rhizobacteria. *Pedosphere* **2024**, *in press*. <https://doi.org/10.1016/j.pedsph.2024.03.005>.
37. Ling, N.; Wang, T.; Kuzyakov, Y. Rhizosphere bacteriome structure and functions. *Nat. Commun.* **2022**, *13*, 836. <https://doi.org/10.1038/s41467-022-28448-9>.
38. Meeds, J.; Kranabetter, J.; Zigg, I.; Dunn, D.; Miros, F.; Shipley, P.; Jones, M. Phosphorus deficiencies invoke optimal allocation of exoenzymes by ectomycorrhizas. *ISME J.* **2021**, *15*, 1478–1489. <https://doi.org/10.1038/s41396-020-00864-z>.
39. Wang, J.; Chen, G.; Ji, S.; Zhong, Y.; Zhao, Q.; He, Q.; Wu, Y.; Bing, H. Close relationship between the gene abundance and activity of soil extracellular enzyme: Evidence from a vegetation restoration chronosequence. *Soil Biol. Biochem.* **2023**, *177*, 108929. <https://doi.org/10.1016/j.soilbio.2022.108929>.
40. Zuccarini, P.; Sardans, J.; Asensio, L.; Peñuelas, J. Altered activities of extracellular soil enzymes by the interacting global environmental changes. *Glob. Change Biol.* **2023**, *29*, 2067–2091. <https://doi.org/10.1111/gcb.16604>.
41. Luo, S.; Phillips, R.P.; Jo, I.; Fei, S.; Liang, J.; Schmid, B.; Eisenhauer, N. Higher productivity in forests with mixed mycorrhizal strategies. *Nat. Commun.* **2023**, *14*, 1377. <https://doi.org/10.1038/s41467-023-36888-0>.
42. Forrester, D.I.; Bauhus, J. A review of processes behind diversity—Productivity relationships in forests. *Curr. For. Rep.* **2016**, *2*, 45–61. <https://doi.org/10.1007/s40725-016-0031-2>.
43. Beidler, K.V.; Taylor, B.N.; Strand, A.E.; Cooper, E.R.; Schönholz, M.; Pritchard, S.G. Changes in root architecture under elevated concentrations of CO₂ and nitrogen reflect alternate soil exploration strategies. *New Phytol.* **2015**, *205*, 1153–1163. <https://doi.org/10.1111/nph.13123>.
44. Wang, Y.; Zi, H.; Li, X. Ectomycorrhizal morphologies and their distribution characteristics in artificial *Populus* forests of eastern and western China. *Acta ecol. Sin.* **2024**, *44*, 1–10. <https://doi.org/10.20103/j.stxb.202403230595>.
45. Guo, L.; Deng, M.; Li, X.; Schmid, B.; Huang, J.; Wu, Y.; Peng, Z.; Yang, L.; Liu, L. Evolutionary and ecological forces shape nutrient strategies of mycorrhizal woody plants. *Ecol. Lett.* **2024**, *27*, e14330. <https://doi.org/10.1111/ele.14330>.
46. Zheng, J.; Freschet, G.T.; Tedersoo, L.; Li, S.; Yan, H.; Jiang, L.; Wang, H.; Ma, N.; Dai, X.; Fu, X.; et al. A trait-based root acquisition-defence-decomposition framework in angiosperm tree species. *Nat. Commun.* **2024**, *15*, 5311. <https://doi.org/10.1038/s41467-024-49666-3>.

Disclaimer/Publisher’s Note: The statements, opinions and data contained in all publications are solely those of the individual author(s) and contributor(s) and not of MDPI and/or the editor(s). MDPI and/or the editor(s) disclaim responsibility for any injury to people or property resulting from any ideas, methods, instructions or products referred to in the content.